Caulerpenyne Binding to Tubulin: Structural Modifications by a Non Conventional Pharmacological Agent

Julien Bourdron[a,b], Pascale Barbier[a,*], Diane Allegro[a], Claude Villard[a], Daniel Lafitte[a], Laurent Commeiras[b], Jean-Luc Parrain[b] and Vincent Peyrot[a]

[a]*INSERM UMR 911 CRO2 ; Aix-Marseille Université, Faculté de Pharmacie, 27 bd Jean Moulin, 13385 Marseille Cedex 05, France;* [b]*UMR-CNRS 6178 SymBio, équipe Synthèse par voie Organométallique, Université Paul Cézanne (Aix-Marseille III), Avenue Escadrille Normandie Niemen, service 532, 13397 Marseille cedex 20, France*

Abstract: The most widely used molecules in cancer chemotherapy are *Vinca*-alkaloids and Taxoids, numerous chemists attempted the synthesis of analogs which bind to their well-known tubulin pharmacological site. Unfortunately, tumors develop resistance to these compounds; therefore the definition of anchoring points and potential binding sites for new drugs on tubulin is of major interest. Caulerpenyne (Cyn), the major secondary metabolite synthesized by the green marine alga *Caulerpa taxifolia* could be one of these drugs, since it inhibits the assembly of tubulin and MTP (Barbier *et al.*, 2001). We observed that the tubulin-Cyn complex is poorly reversed. Cyn did not bind to sulfhydryl groups and the measure of the extent of binding is 1.6 ± 0.2 suggesting two potential binding sites. Then, we demonstrated by competition measurements that Cyn did not interact to colchicine, Taxol® and *Vinca*-alkaloid binding domain. Finally, mass spectrometric analysis of proteolytic cleavage of tubulin-Cyn complex demonstrated that Cyn did not bind covalently to tubulin and evidenced two good candidate regions for Cyn binding, one on α-tubulin and the other on β-tubulin.

Key Words: Tubulin, caulerpenyne, MALDI-TOF, microtubule, electrospray.

INTRODUCTION

Most algae of Caulerpales order live in tropical area. *Caulerpa Taxifolia*, a marine tropical alga was introduced in the Mediterranean in 1984 [1]. For 20 years, it colonizes several thousands hectares along Mediterranean coast. From this alga nine secondary metabolites were isolated [2] bearing a common functional group, the terminal 1,4-diacetoxybutadiene moiety responsible of their biological activity [3]. Our study focus on the principal one, caulerpenyne (Chart **1**), which has been first isolated from the Mediterranean alga *C. prolifera,* [2]. Caulerpenyne has antibacterial and antineoplastic activities [4]. It alters ATP-dependent Ca^{2+} storage in intracellular organelles, protein phosphorylation, and DNA synthesis [5]. Its cytotoxicity has been demonstrated in several tumor cell lines [6,7]. Caulerpenyne inhibits SK-N-SH cell proliferation without any blockage in G2/M phase and enhances cell death. In this cell line, caulerpenyne induces a loss of neurites and a compaction of the microtubule network at the cell periphery [7]. These modifications are unique and not observed with the classical antimitotic agents, which stabilize or disrupt microtubule formation. Among these agents, taxoids stabilize microtubules into non-functional bundles [8] whereas *Vinca*-alkaloids disassembled microtubules and induced the formation of paracrystals at higher concentrations [9]. Moreover, caulerpenyne induces the inhibition of microtubule assembly [7]. There are two major differences, between caulerpenyne and classical microtubule inhibitors. First, the half inhibitory concentrations of caulerpenyne (51 μM for MTP: tubulin plus microtubule-associated proteins and 20 μM for pure tubulin) are much higher than those of colchicine, podophyllotoxin, vinblastine, or dolastatin 10 [10-13]. Second, pre-incubation with the protein is necessary to obtain an effect. However, Caulerpenyne induces a large cold-irreversible aggregation of tubulin and bundling of microtubules, as demonstrated by electron microscopy [7]. This aggregation is not limited by the presence of microtubule associated proteins in the case of MTP assembly and it is reminiscent of microtubule bundling described *in vitro* [14]. Moreover, (–)-caulerpenyne (Cyn) the synthetic isomer of natural (+)-caulerpenyne shows an inhibitory effect of microtubule assembly *in vitro* with a half inhibitory concentration of 14 ± 2 μM [3].

To understand the mechanism of action of the new pharmacological agent caulerpenyne, we performed turbidimetry, fluorescence spectroscopy and analytical ultracentrifugation experiments on tubulin-cyn complex in presence of colchicine, *Vinca*-alkaloids analogues and taxol®. As shown by gel filtration assay two Cyn molecules bind to α–β tubulin dimer; the two candidate regions for Cyn binding, distinct from known anti-tubulin agents, were determined by MALDI-TOF and nano LC ESI mass spectrometry. One is on α-tubulin and the other on β-subunit.

RESULTS

Cyn Binding: Sulfhydryl Groups and Extent of Binding to Tubulin

Microtubule formation is inhibited by inorganic sulfhydryl blocking agent such as *cis*-dichlorodiamine-platinum

*Address correspondence to this author at the INSERM UMR 911 CRO2 ; Aix-Marseille Université, Faculté de Pharmacie, 27 bd Jean Moulin, 13385 Marseille Cedex 05, France; Tel: +33 4 91 83 56 16; Fax: +33 4 91 83 55 05; E-mail: pascale.barbier@pharmacie.univ-mrs.fr

1573-4064/09 $55.00+.00

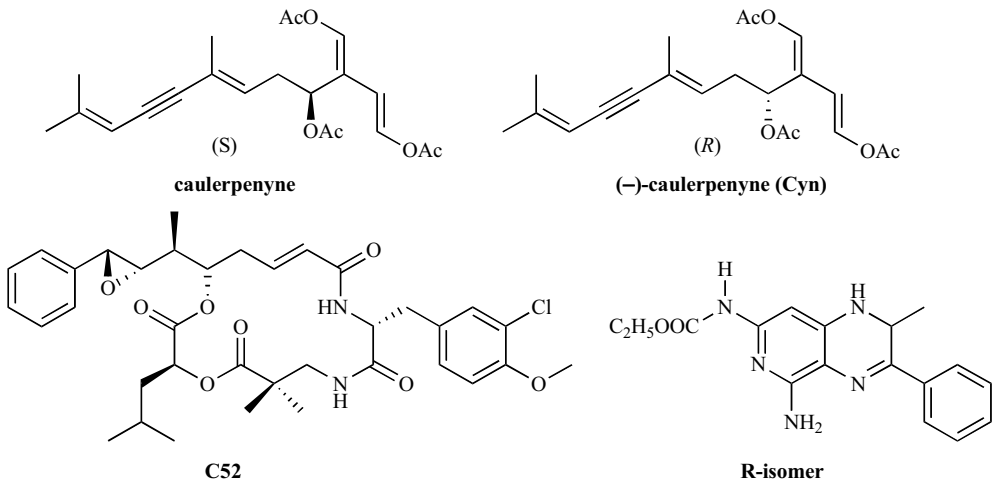

Chart 1.

[15], oxaliplatin (P. Barbier personal data) and arsenic trioxide [16]. In these cases, tubulin and ligand are incubated at 37°C to observe their microtubule formation inhibitory effects *in vitro*. With Cyn, similar behavior was observed so we suspected a possible covalent binding of Cyn to free sulfhydryl groups of tubulin. Tubulin, a heterodimeric protein ($\alpha\beta$), has 20 cysteine residues, 12 in the α subunit and 8 in the β subunit, some of them are directly involved in the assembly process [17; 18]. In the present study, the number of sulfhydryl groups measured was 19.00 ± 0.20 per tubulin dimer. In presence of five to ten fold excess of Cyn, this number became 18.80 ± 0.20 even after 24h of incubation between Cyn and tubulin. Consequently, the binding of Cyn did not involve the sulfhydryl groups of tubulin.

Binding of Cyn to tubulin seems to be a slow complex phenomenon (an incubation time is necessary between Cyn and tubulin to inhibit the formation of microtubule), not easily reversed. Indeed after a gel filtration (Sephadex G25) of a tubulin-Cyn complex, the polymerization process could not be recovered (data not shown). Therefore, we used this later characteristic of tubulin-Cyn complex to study the interaction between tubulin and Cyn. We examined by a gel filtration assay depicted in Materials and Methods the extent of the binding of Cyn to tubulin. In presence of an excess (from three to ten) of Cyn, the binding was characterized by mole of bound ligand / mole of total tubulin (ν) value of 1.60 ± 0.20. This indicates that Cyn has two potential binding sites to tubulin.

Cyn Binding and Taxol®-Induced Microtubule Formation

Fig. (**1A**), shows typical microtubules obtained with the tubulin-Cyn complex in presence of stoichiometric amount of Taxol®. The determination of the critical concentration (Cr) of tubulin necessary to form microtubules with Taxol® in absence and in presence of Cyn is depicted in Fig. (**1B**). The values were Cr = 1.1 ± 0.9 $mg.mL^{-1}$ and Cr = 1.7 ± 0.9 $mg.mL^{-1}$ for tubulin and tubulin-Cyn complex, respectively. Then, samples were centrifuged and the pellet and the supernatant were analyzed by SDS-Page electrophoresis, to determine the concentration of microtubule and free tubulin (Fig. (**1C**)) For all samples, we did not observe any difference between pellet and supernatant, indicating that Cyn did not disturb the Taxol® tubulin assembly process. These results suggest that Cyn binding to tubulin does not affect the interaction of Taxol®.

Cyn Binding and Vinca-alkaloïd Domain

Cryptophycin 52 (C52) which binds to the tubulin *Vinca*-alkaloïds site is known to induce ring-shaped oligomers dependent on protein and drug concentration [19]. These oligomers, composed of 9 tubulin dimers, were quantified by analytical ultracentrifugation sedimentation velocity experiment. We used this method to validate that whether Cyn binds to the same domaine as C52, the ring formation should be inhibited. Fig. (**2A**) shows the sedimentation coefficient distribution of tubulin (10 μM) with and without an excess of Cyn. The apparent sedimentation coefficient (S_{app}) of tubulin dimer was found identical in both cases and equal to 5.04 ± 0.01 S. The only difference observed was the increase (14%) in the amount of tubulin aggregation with an apparent sedimentation coefficient of 8-9 S. This is consistent with our previous results where we showed that Cyn induced tubulin aggregation responsible for inhibition of microtubule formation and bundling of residual microtubules [19]. Fig. (**2B**) represents similar experiment with C52. In this case, tubulin (dark line) sedimented as a single species at a sedimentation coefficient 15 S with a slight spreading shoulder at about 8-9 S. In presence of Cyn (dashed line) similar profile was observed with a slight decrease in the 15 S compensated by a slight increase in the 8-9 S amount. This observation is in agreement with the increase of tubulin aggregation always found in presence of Cyn. In conclusion, in presence of Cyn, C52 binds to tubulin and induces its self-association into rings suggesting that these two molecules do not share the same binding domain.

Cyn Binding and Colchicine Domain

Two isomers of ethyl-5-amino-2-methyl-1,2-dihydro-3-phenylpyrido[3,4-*b*]pyrazin-7-yl carbamate were extensively studied in our laboratory [20-26]. Their binding on colchicine site induces a quenching of tubulin tryptophanyl residues and an increase of ligand fluorescence by energy transfer. We used the increase of R-isomer fluorescence to deter-

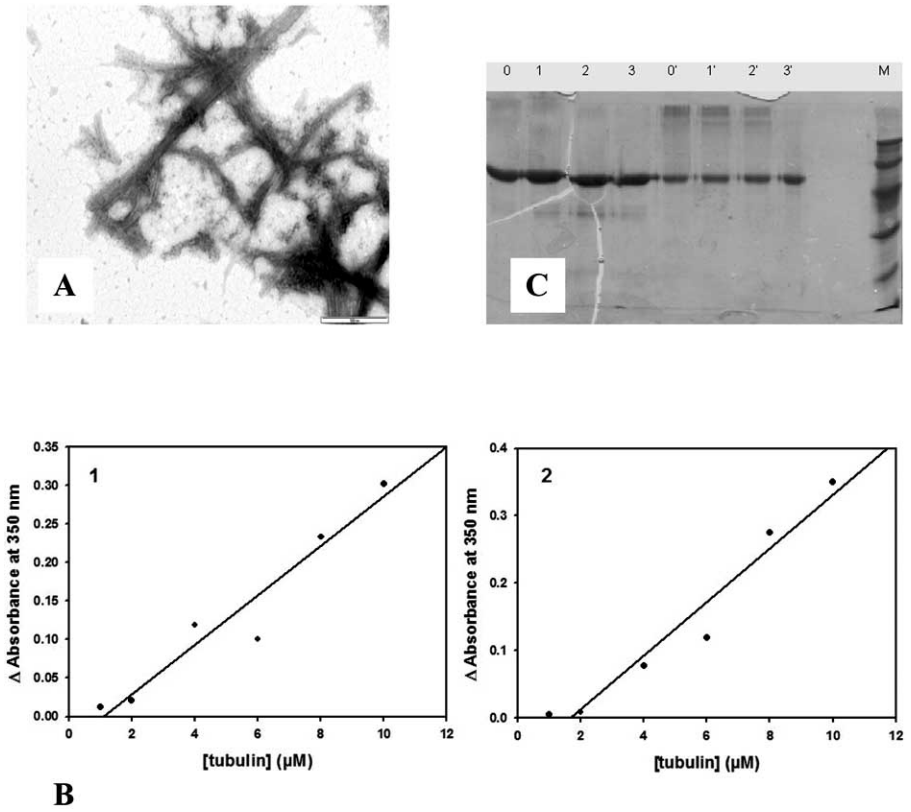

Fig. (1). A- Electron microscopy of tubulin-Cyn in the presence of Taxol® and with 8 mM Mg^{2+}, showing microtubules and bundled microtubules. The bar represents 500 nm. **B-** Plateau absorbance values as a function of the total tubulin concentration, tubulin alone (**1**) and in the presence of Cyn (**2**) **C-** SDS-Page Gel electrophoresis analysis of the assembly induced by Taxol®: Pellets; lane 0 tubulin alone (15 μM), lanes 1, 2, 3 tubulin with 50, 60, 120 μM Cyn. Supernatants; 0' tubulin alone, lanes 1', 2', 3' with 50, 60, 120 μM Cyn. M is the molecular mass marks.

mine its affinity binding constant to tubulin and tubulin-Cyn complex. The data shown in Fig. (**3**) were analyzed as described in Barbier *et al.*, [22]. We obtained an affinity constant of $(3.0 \pm 0.5) \times 10^6$ M^{-1} for tubulin and an affinity constant of $(3 \pm 1) \times 10^6$ M^{-1} for the Cyn-tubulin complex (mean of three independent experiments). The presence of Cyn does not modify the affinity constant of R-isomer indicating that Cyn does not bind to colchicine domain.

With the results described above, we postulate that Cyn could interact with tubulin on area distinct than Taxol®, *Vinca*-alkaloids and colchicine binding domains.

Cyn Binding and Effects to the Structure of Tubulin

Mass spectrometry coupled with tryptic digestion was used to analyze the conformational consequences of Cyn binding to tubulin. First, we realized similar experiments and analysis with the perfectly characterized tubulin-colchicine complex. The crystallographic data (available in PDB, 1SA0) of the structure, at 3.5 Å resolution, of tubulin in complex with colchicine and with the stathmin-like domain (SLD) of RB3 has been determined and the colchicine binding site localization has been specified [27]. A comparison with the structure of tubulin in protofilaments shows changes in the subunits of tubulin as it switches from its straight conformation to a curved one. Moreover, the tubulin–colchicine complex sheds light on the mechanism of colchicine's activity: colchicine binds to a location where it prevents curved tubulin from adopting a straight structure, which inhibits assembly. By using PDBsum we compared the α–β intradimer contacts between 1FFX (tubulin in complex with the stathmin-like domain without colchicine) and 1SA0 (tubulin liganded with colchicine and stathmin-like domain). Then, we generated a molecular model showing the supplementary contacts generated by the binding of colchicine to a tubulin dimer (Fig. (**4A**)). All of the contacts were located on the α-tubulin side and near colchicine molecule in β-tubulin, and they changed the α–β intradimer contacts. Since Colchicine binding to tubulin is almost irreversible we could envision that ligand binding to tubulin will disturb tryptic digest. Therefore tubulin and tubulin-colchicine complex were digested with trypsin. Tryptic peptides were identified by MS/MS and profiles were compared using MALDI TOF analysis (Fig. (**5**)). The Mass spectrometric signal corresponding to several tryptic peptides showed a marked difference in intensity between the two conditions. These peptides were located on α-tubulin: residues 84-105, 229-243, 308-320 and on β-tubulin: residues 218-243 and 326-352. The meaning of a modification in intensity of a tryptic peptide is that the accessibility of K and R, the target amino acids of trypsin, is modified. The caveat is that it is quite difficult to know whether accessibility is modified at one end of the peptide or the other or on another K or R if the peptide is miscleaved. All K and R candidates are given in Table **1**. In

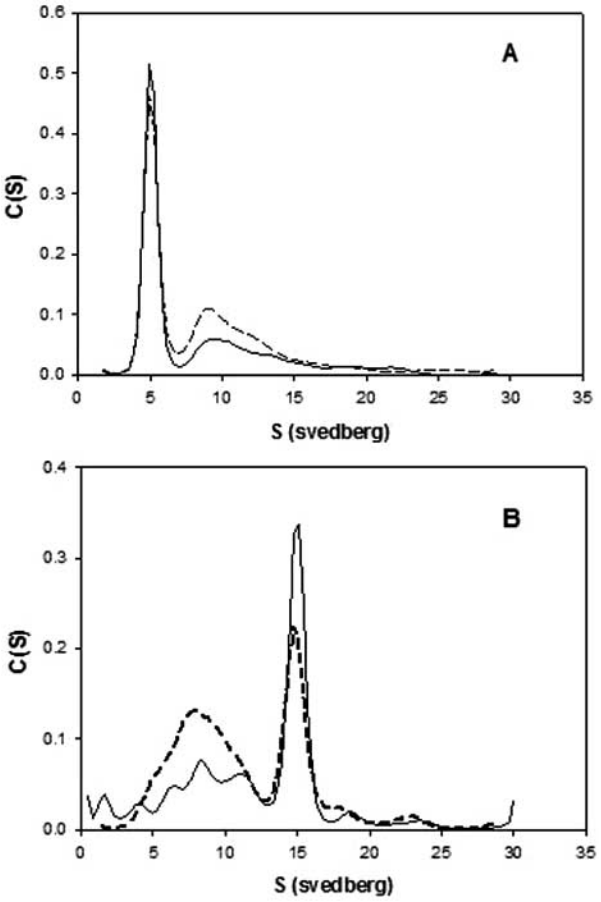

Fig. (2). (A) Sedimentation coefficient distribution C(S) of tubulin (10 μM) in presence (dashed line) or in absence (line) of an excess of Cyn. **(B)** Similar experiment in presence of 50 μM of C52. The increase of species centered at 15S indicates C52 induced ring.

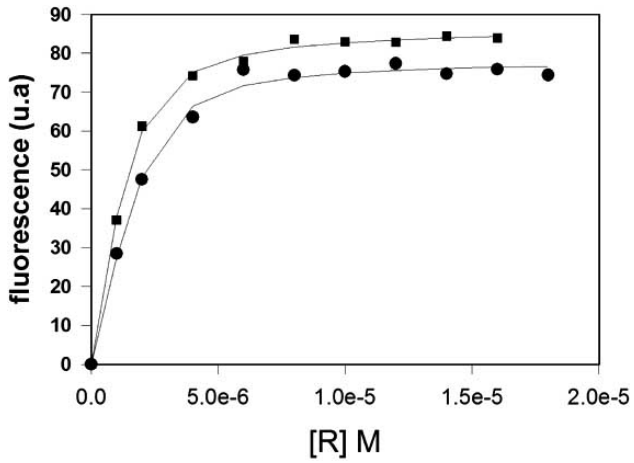

Fig. (3). Fluorometric titration (emission at 460 nm) of 5 μM tubulin (square) and 5 μM tubulin-Cyn complex ((black dot) with various concentrations of the R-isomer. The solid line is the fit obtained as described in Materials and Methods.

presence of colchicine, MS analysis revealed that as expected protein digestion is modified on the vicinity of the drug binding site (Fig. (**4B**)) and also provides additional modifications compared to X-ray analysis (Fig. (**4A**)) in α– and β–tubulin. These modifications are probably coming from allosteric modifications of the structure due to ligand binding. The same analysis was conducted for tubulin-Cyn complex. Peptide mass finger printing at 1h, and 16h of tubulin-cyn complexes were similar with peaks obviously different from the digest of the tubulin alone. This is in agreement with a slow dissociation process of the ligand. Comparison between the two samples revealed that Cyn disturbed the accessibility of trypsin to various peptides in α-tubulin: 229-243, 244-264, 308-320, 390-401, 402-422 and 1-19, 20-48, 63-103, 105-123 in β-tubulin (Fig. (**4C**)). However, we did not detect masses corresponding to tubulin peptides with Cyn or Cyn fragments, caulerpenyne binding to tubulin is probably non covalent. Careful examination of the results (Table **1**) is helpful to distinguish between a potential binding site and allosteric modification of the structure. First, R229, R243, R308, K310 and R320 (all in α-tubulin) could be disturbed in both complexes (tubulin-colchicine and -Cyn). These results suggested some steric effects due to protein stabilization by formation of a protein-ligand complex; this trivial effect is independent of the ligand nature. Therefore, these residues do not contribute to the ligand binding site. Second, the modifications of K96 and R105 of α-tubulin and K326 in β-tubulin in presence of colchicine are known to be implicated in regular intradimer contacts without any ligand. Similar results are obtained for K401, R402 in α-tubulin and for R2 in β-tubulin in presence of Cyn. Disturbed lysines and arginines *via* potential close contacts with Cyn were focused in two areas, one in α-tubulin (R264, R390, K394 and R422) and the other in β-tubulin (K19, R48, R79, R88, K105 and R123). These two regions are good candidates for the binding site of Cyn. Moreover, this result is in good agreement with the fact that Cyn has an extent of binding equal to 1.6.

DISCUSSION

(+)-Caulerpenyne, the major metabolite from *Caulerpa taxifolia*, inhibits microtubule assembly related to an antiproliferative activity on cell line SK-N-SH [7]. Cyn ((–)-caulerpenyne), a synthetic isomer of caulerpenyne, share the same effect on microtubule assembly, more important than observed with (+)-caulerpenyne [3]. The aim of our work was to understand the mechanism of binding between Cyn and tubulin.

Drugs which require preincubation to inhibit assembly of tubulin often bind to sulfhydryl groups. Cyn need incubation with tubulin, however we found no difference between the numbers of free sulfhydryl groups on tubulin and tubulin-Cyn complex even after 24 hours incubation. Consequently, Cyn does not react with thiol groups available on tubulin.

With competition experiments we examined the influence of Cyn on *Vinca*-alkaloids and Colchicine analogues and Taxol® binding to tubulin. Indeed, these three classes of drugs are the most studied anti-microtubules molecules; they are perfect tools to investigate drug action on microtubules functions. As seen in the results section the competition measurements with the R-isomer suggest that Cyn does not overlap fully or partially the R-isomer site. As C52 binds to tubulin in the vicinity of *Vinca*-alkaloid binding site [28-30], we decided to compare Cyn and C52 binding. It is well

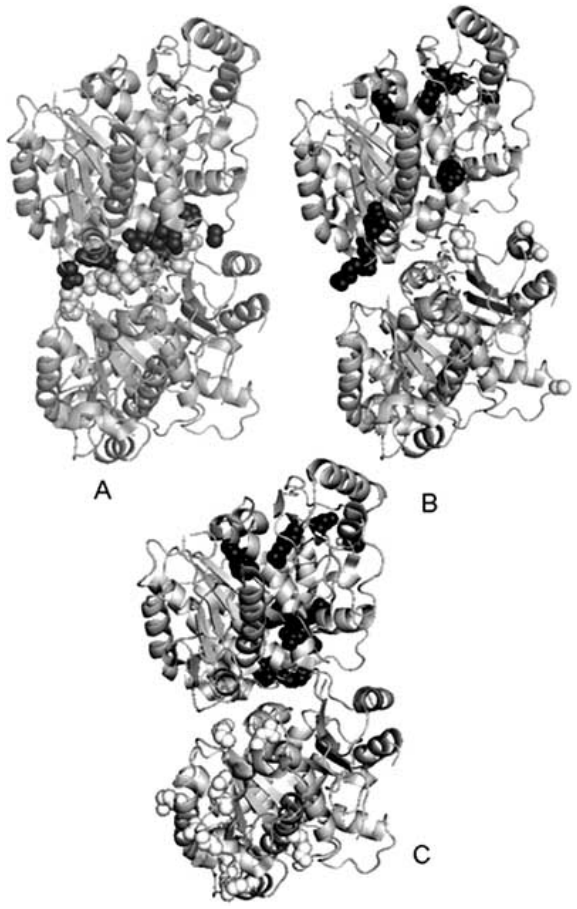

Fig. (4). This figure was prepared with PYMOL. **A**: Comparisons between 1FFX (without colchicine) and 1SA0 (with colchicine), the modified residues are in black balls for α-tubulin, in grey balls for β–tubulin, DAMA-Colchicine is in CPK mode. **B**: Mass spectroscopy study, comparison between tubulin and tubulin-colchicine complex, only R (black balls) and K (grey balls) residues are shown. **C**: Mass spectroscopy study, comparison between tubulin and tubulin-Cyn complex, only R (black balls) and K (grey balls) residues are mentioned.

known that the binding of C52 depends on tubulin concentration, and induces changes in the sedimentation pattern of tubulin, which indicates that Cryptophycin 52 self-associates tubulin in ring-shaped oligomers [19, 31]. In presence of Cyn, we observed a decrease of 14 % in the amount of ring-shaped oligomers and an increase of 16 % of tubulin aggregation. This increase in aggregation in presence of Cyn is also observed in absence of C52. So, binding of Cyn induced a partial (mean of 15%) aggregation of tubulin which then could mask the C52 binding site located in the interface between α and β subunit of two adjacent tubulin dimers. Cyn binding domain do not overlap the *Vinca*-alkaloïd one, however the aggregative potential of Cyn could decrease *Vinca*-alkaloïd binding on tubulin.

It has been clearly demonstrated that colchicine binding to tubulin decrease the polymer stabilizing capacity of Taxol® [32]. Therefore, it was very tempting to study the effects of Cyn binding to tubulin in presence of Taxol®. Cyn does not affect the tubulin assembly process in presence of Taxol® this indicating that Cyn does not overlap the stabilizing agent site. The fact that Taxol® overcomes the inhibitory activity of Cyn indicates that Taxol® reduces the steric hindrance and the geometric strain generated by Cyn binding to tubulin.

In summary our work highlights that Cyn could have two potential binding sites. By competition measurements we found that Cyn binding does not significantly implicate the colchicine, *Vinca*-alkaloïds and Taxol® binding domains. The unique explanation is that this new pharmacophore (the terminal 1,4-diacetoxybutadiene moiety of caulerpenyne analogues) generate new productive contacts with loci in tubulin not involved in binding sites of the major antimitotic drugs.

Since all the main antimitotic drugs induce structural change in tubulin, we examine the consequences of Cyn binding to tubulin by mass spectroscopy. Native tubulin and tubulin-Cyn complex were proteolyzed under identical conditions by trypsin and proteolytic fragments were analyzed by MALDI-TOF and nano LC ESI-MS/MS. Cyn binding induces new cleavage points in α- and β-tubulin (Table **1**). The 3D maps of the proteolytic nicking points in presence of Cyn permit to define two extend zones: one in the C-terminal domain of the α-tubulin and the other in the N-terminal domain of β-tubulin. These two regions (Fig. (**6**)) do not overlap the colchicine, *Vinca*-alkaloids and Taxol® binding sites which are in good agreement with the competition experiments.

Since, *Vinca*-alkaloids and Taxoids molecules are extremely important in cancer chemotherapy, numerous chemists attempted the synthesis of analogs which binds to their well-known tubulin pharmacological site. Unfortunately, tumors develop resistance to these drugs; it explains why the definition of new anchoring points and potential binding sites for new drugs on tubulin is crucial. Recently, Yoshida *et al.* [33] showed that pironectin, a natural compound isolated from *streptomyces* covalently binds to α-tubulin at Lys352, and is effective not only against human tumor cell lines resistant to microtubule-targeted drugs, but also on multidrug-resistant cells with mdr1 gene expression [33]. In the same way, dicoumarol, an anticoagulant molecule, binds to tubulin in an unknown site different than that of standard antimicrotubule agent, stabilize microtubule and is synergistic with Taxol® [34]. Our results with Cyn strengthen the idea that developing new molecules which bind to other pharmacological sites than Taxol^R and *Vinca*-alkaloids on tubulin is important. Such drugs could be combined in cancer chemotherapy.

EXPERIMENTAL SECTION

Drugs

(−)-caulerpenyne (Cyn) was synthesized as previously described by Commeiras *et al.* [3], dissolved in dimethylsulfoxide (Me_2SO) and stored at -20°C. Cyn concentrations were measured spectrometrically in ethanol, with an extinction coefficient of 31000 $M^{-1}.cm^{-1}$at 252 nm [2]. Cryptophycin 52 (C52) was a gift from Eli Lilly and Co., through the courtesy of Dr. Dan Williams, and was used without further purification. Its concentration was determined spectrometrically using an extinction coefficient of 2132 $M^{-1}.cm^{-1}$ at 280

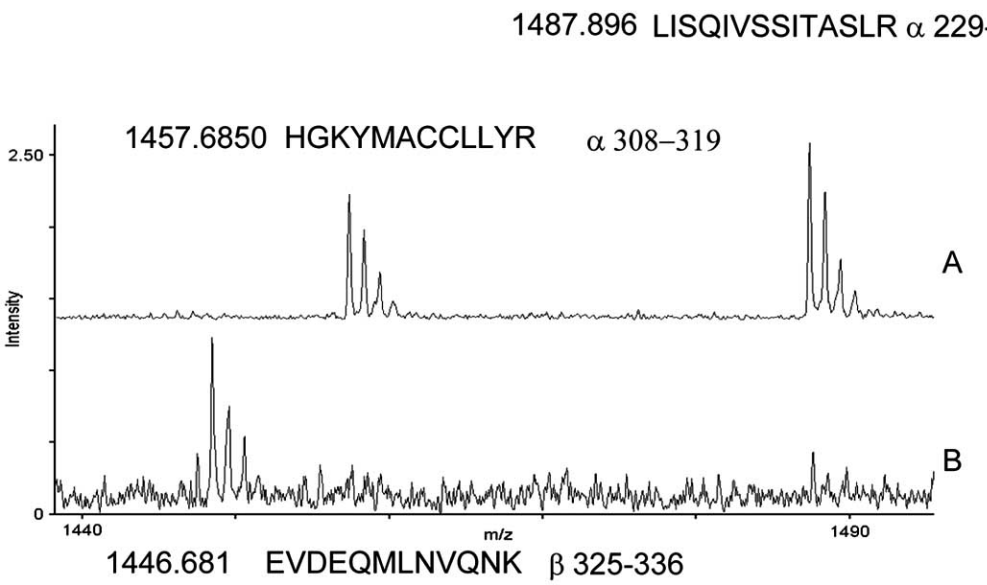

Fig. (5). Peptide mass fingerprinting obtained by MALDI TOF of tubulin (**A**) and tubulin-colchicine complex (**B**).

nm [19]. NSC 613863 was a gift of Dr A. Rener [35] and we measured its concentration using an extinction coefficient of 15400 $M^{-1}.cm^{-1}$ at 374 nm. Taxol^{R} was purchased from Sigma (St Louis, MO). All the solutions were prepared in Me_2SO and stored at – 20 °C. The molecule structures are shown in chart 1. All other reagents are analytical grade.

Tubulin Purification and Microtubules Assembly

Lamb brain pure tubulin was purified from brain soluble extract by modified Weisenberg procedure consisting in ammonium sulfate fractionation and ion exchange chromatography [36]. Then, pure tubulin was stored in liquid nitrogen and prepared for use as described [37, 25]. Tubulin concentration was determined spectrometrically at 275 nm in 6

Table 1. Comparison Between Tubulin and Tubulin-Colchicine and -Cyn Complexes. We only note the R and K Residues Implicated in the Structural Changes. In Black R and K Residues Implicated in Regular Intradimer Contacts Between α–Tubulin and β–Tubulin, Revealed by the Binding of Colchicine or Cyn. (*) Accessibility of Amino-Acid Residues Modified by Both Ligands. The 3D Structure of α–β Tubulin Dimer Shows that *R 264* is Near Residues *R390, K394, K401, R402, R422* Located in the C-ter Domain of α-Tubulin. The Underlined Amino-Acid Residues are Closed Together in the N-ter Domain of β-Tubulin.

	In PDB Code 1SA0 Tubulin liganded with Colchicine *vs.* 1FFX Tubulin without Colchicine	Mass Spectroscopy Tubulin *vs.* Tubulin-Colchicine	Mass Spectroscopy Tubulin *vs.* Tubulin-Cyn
α-tubulin	R 221 K 401	R 84 ***K 96*** ***R 105*** R 229* R 243* R 308* K 311* R 320*	R 229* R 243* ***R 264*** R 308* K 311* R 320* ***R 390*** ***K 394*** ***K 401*** ***R 402*** ***R 422***
β-tubulin	R 164 K 352	K 218 R 243 **K 326** K 338 K 352	**R 2** K 19 R 48 R 79 R 88 K 105 R 123

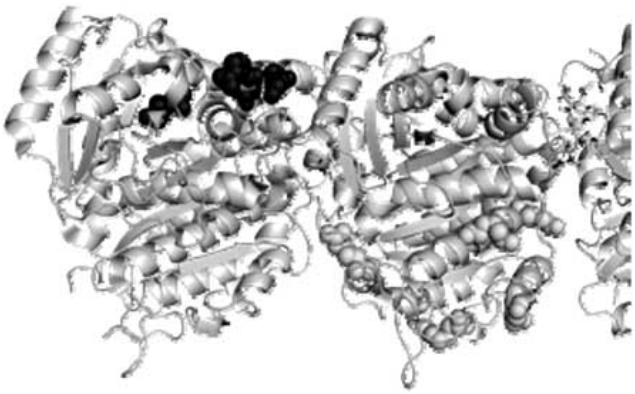

Fig. (6). Molecular modelling showing the two regions modified by the binding of Cyn to tubulin. Protein originates from X-ray structure of its complex with DAMA-colchicine (between α-and β-tubulin) and with vinblastine (encoded as 1Z2B in PDB). The α– and β-tubulin (from left to right) was in grey ribbon representation. R and K residues represented by black balls were located on the C-ter region of α-tubulin (CPK mode). R and K residues represented in grey balls were located mainly on the N-ter region of β-tubulin (CPK mode). This figure was prepared with PYMOL.

M guanidine hydrochloride ($E_{275\ nm}$ = 1.09 $L.g^{-1}.cm^{-1}$) or in 0.5 % sodium dodecyl sulfate in neutral aqueous buffer ($E_{275\ nm}$ = 1.07 $L.g^{-1}.cm^{-1}$). The buffer solution used to form microtubules from pure tubulin consisted of 20 mM sodium phosphate, 1 mM EGTA, 3.4 M glycerol, 0.1 mM GTP and 1 mM $MgCl_2$, pH 6.9. After 35 min of incubation at 37 °C with Cyn or Me_2SO (control), the tubulin assembly was started by addition of 9 mM $MgCl_2$ in a thermostated cuvette (1 x 0.2 cm), and the mass of polymer formed was monitored by turbidimetry at 350 nm in a Beckman DU 7400 spectrophotometer. To determine the inhibitory effect, we calculated the difference between the polymerization plateau value and the depolymerization plateau value and expressed it in percentage of inhibition relative to the control.

Taxol® induced microtubule formation are done in 20 mM sodium phosphate buffer, 0.1 mM GTP, pH 7. Tubulin with Cyn or Me_2SO (control) was first incubated 35 min at 37 °C. Then microtubules formation was induced by adding 8 mM of $MgCl_2$ and a stoichiometric Taxol® concentration, the mass of polymer formed was monitored by turbidimetry and SDS-Page analysis. Taxol®-induced microtubules at different concentrations of tubulin with and without Cyn were centrifuged at 125000 g during 8 min in a Beckman airfuge® ultracentrifuge. The pellet and the supernatant (representing the tubulin critical concentration for microtubule formation) were then analyzed by SDS-Page.

Free Tubulin Sulfhydryl Concentration Determination

Determination of free SH on tubulin with DTNB (Sigma) was used as described by Peyrot *et al.* [15]. After 35 min of incubation at 37°C, 0.1 mL tubulin (15 µM) with and without 50 µM of Cyn solutions are mixed with 0.9 mL of a buffer containing 20 mM NaPi, 6.4 M urea, 1 mM of DTNB, pH 7.5. The formation of the thio-nitrobenzoate anion induced by DTNB reaction on the tubulin free sulfhydryl group was measured at different times (0, 1 and 24 hours) by absorbance at 412 nm using an extinction coefficient of 13600 M^{-1} cm^{-1}.

Sedimentation Velocity

The experiments were done at 40 000 rpm and 20 °C in a Beckman Optima XL-A analytical ultracentrifuge equipped with absorbance optics, using an An55Ti rotor and 1.2 cm Epon double-sector centerpieces. Apparent sedimentation coefficients were determined by the sedimentation coefficient distribution C(S) generated by SEDFIT program [38].

Binding Measurements by Fluorometric Titration

The increase in NSC613863 ligand fluorescence due to its interaction with tubulin was employed to estimate its binding parameters in presence of Cyn. Tubulin or tubulin-Cyn complex were titrated with various concentrations of NSC613863. The fluorescence measurements were performed with a Perkin-Elmer Luminescence Spectrometer 50 with slit widths of 5/5 nm monitored by an IBM PS2 computer. Uncorrected fluorescence spectra were obtained by using 0.2 (excitation) x 1 cm cells (Hellma) thermostated at 25 °C by a circulating water bath. Emission spectra (λ_{exc} = 380 nm) was collected. After correction for the inner filter effect, the fluorescence intensity values at 460 nm were plotted versus R-isomer concentrations, and the binding parameters fitted as described elsewhere in Barbier *et al.* [22].

Electron Microscopy

Samples were adsorbed onto 200 mesh Formvar carbon-coated copper grids, stained with 2% (w/v) uranyl acetate, and blotted to dryness. Grids were observed using a JEOL JEM-1220 electron microscope operated at 80 kV.

Measurements of the Stoichiometry of CYN to Tubulin by a Gel Filtration Assay

Various concentrations of Cyn (30-50 µM) with tubulin (4-10µM) were incubated 35 min at 37 °C in 20 mM sodium phosphate buffer pH 7. Then, 500 µL of each samples (with and without Cyn) were applied to and eluted through a Sephadex G25 column (1 x 15 cm) at a constant flow rate with the same buffer. Absorbance measurements of the collected fraction (500µL) were done at 252 nm in presence of Cyn and at 276 nm for tubulin alone. Tubulin concentrations were calculated with an extinction coefficient of 1.16 $Lg^{-1}cm^{-1}$ (scattering-corrected absorbance in a neutral aqueous buffer). The absorbance measurements at 252 nm were corrected for the contribution of tubulin and then Cyn concentrations were calculated using the above extinction coefficient of 31000 $M^{-1}.cm^{-1}$at 252 nm.

Mass Spectrometry

Tubulin-colchicine complex was prepared as described [39]. The dissociation of tubulin-colchicine complex is a single first-order process with a net rate constant of 3.37 x 10^{-6} s^{-1} at 25 °C [40]. Over the time of duration of the experiments (1h) less than 2% of the initial complex was dissociated. Thus the complex can be considered as "irreversible". The tubulin-Cyn complex was prepared by incubation 35 min at 37 °C of tubulin (80 µM) with Cyn (200 µM), the

complex was then passed through a Sephadex G25 chromatography to remove the free Cyn and Cyn-tubulin aggregates. The complex was diluted to obtain a tubulin concentration of 1 µM. Tryptic digestion and MALDI-TOF was performed as described. 100 µL of 0.1 mg/mL of tubulin samples with or without ligand were digested for 15min, 30 min, and 1 hour or overnight (16 hours) using sequencing grade modified porcine trypsin (12.5 ng/µL, Promega, Madison, WI). The peptides were extracted, dried in a vacuum centrifuge, and resuspended in 20 µL of 0.1% TFA. The peptide mixture resulting from proteins digestion was analyzed using an Ettan pro MALDI time-of-flight mass spectrometer (Amersham Biosciences, Uppsala, Sweden) in positive ion reflector mode. 0.5 µL of the peptide mixture was cocrystallized on the MALDI target with an equal amount of matrix solution (5 mg/mL of α-cyano-4-hydroxycinnamic acid in 50% acetonitrile) in the presence of 0.5 % TFA. 500 laser shots were averaged to obtain the final spectrum. Spectra were normalized on the highest peak using the origin software. Spectra with and without ligand were then compared using the progenesis software (Nonlinear Dynamics Ltd, Newcastle upon Tyne, UK). Three independent sets of experiments were analyzed. Peaks where compared using a simple subtractive method: when peak height differed by at least 3 times and in the three independent sets of experiment This drastic value (none of the peak intensities in two similar experiments varied by more than 30%) avoid false positives and only considered the most significant differences due to ligand binding.

LC-MS data sets were acquired with a liquid chromatograph (Ettan multi dimensional liquid chromatography (Amersham biosciences) and electrospray ionization quadrupole ion trap mass spectrometer (LCQ deca XPplus, Thermo Finnigan, San Jose, CA). nano-scale chromatographic separations were performed with a reversed-phase column (Agilent, Zorbax 300SB C18, 150 × 0.075 mm column 3.5 µm) and binary solvent system made up of 0.1% formic acid (solvent A) and acetonitrile, 0.1% formic acid (solvent B). A linear gradient program was used that changed the composition of solvent from 0% B to 46% B over a 90-min period at a constant flow rate of 200 nL/min. An injection volume of 2 µL was used. Positive mode nano electrospray ionization was performed using a capillary temperature of 200 °C, a source voltage of 1.8 kV, a capillary voltage of 45 V, and a maximum injection time of 200 ms. The LCQ was calibrated using the manufacturer's tuning solution and tuned to optimize the response of the ion at *m*/*z* 1046, which is derived from the angiotensin II peptide. Full-scan mass spectra were acquired over an *m*/*z* range of 400-1800 Da. Targeted MS/MS analysis was performed using an isolation width of 2.5 *m*/*z* units and a relative collision energy of 35%. Tandem mass spectra were directly submitted to bioworks (Thermo Finnigan, San Jose, CA) or mascot searches for protein identification using the NCBI nr database.

Analysis of the 3D structures was done with PDBsum (http://www.ebi.ac.uk/thornton-srv/databases/pdbsum/) which provides an at-a-glance overview of every macromolecular structure deposited in the Protein Data Bank (PDB), giving schematic diagrams of the molecules in each structure and of the interactions between them.

ACKNOWLEDGEMENT

We are grateful to R. Michel (INSERM UMR911) for his technical assistance. Julien. Bourdron thanks DIPTA Company and La region PACA for financial support.

ABBREVIATIONS

Cyn	=	(−)-caulerpenyne
C52	=	Cryptophycin 52
DTNB	=	5, 5'-dithio-bis(2-nitrobenzoate)
MAPs	=	Microtubule-associated proteins
Me_2SO	=	Dimethyl sulfoxide
MTP	=	Tubulin plus microtubule-associated proteins
PDB	=	Protein Data Bank (http://www.rcsb.org/pdb/)
PG buffer	=	20 mM sodium phosphate-0.1 mM GTP, pH 7.0
MS/MS	=	Tandem Mass Spectrometry
ESI	=	Electrospray Ionization
LC	=	Liquid Chromatography
maldi-TOF	=	Matrix Assisted LASER desorption/Ionization-Time Of Flight

REFERENCES

[1] Meinesz, A.; Hesse, B. Introduction et invasion de l'algue tropicale *C. taxifolia* en Méditerranée Nord-Occidentale. *Oceanol. Acta*, **1991**, *14*, 415.

[2] Amico, V.; Oriente, G.; Piatelli, M.; Tringali, C.; Fattorusso, E.; Magno, S.; Mayol, L. Caulerpenyne, an unusual sesquiterpenoid from green alga *Caulerpa prolifera*. *Tetrahedron Lett*., **1978**, *38*, 3593.

[3] Commeiras, L.; Bourdron, J.; Douillard, S.; Barbier, P.; Vanthuyne, N.; Peyrot, V.; Parrain, J.L. Total Synthesis of Terpenoids Isolated from Caulerpale Algae and Their Inhibition of Tubulin Assembly. *Synthesis*., **2006**, *1*, 166.

[4] Hogson, L.M. Antimicrobial and antineoplastic activity in some south Florida seaweeds. *Botanica Marina,* **1984**, *27*, 387.

[5] Lemée, R.; Pesando, D.; Durand-Clément, M.; Dubreuil, A.; Meinesz, A.; Guerriero, A.; Pietra, F. Preliminary survey of toxicity of the green alga *C.taxifolia* introduce into Mediterranean. *J. Appl. Phycol.,* **1993**, *5*, 485.

[6] Fischel, J.L.; Lemée, R.; Formento, P.; Caldani, C.; Moll, J.L.; Pesando, D.; Meinesz, A.; Grelier, P.; Pietra, F.; Guerriero, A.; Milano, G. Cell growth inhibitory effects of caulerpenyne, a sesquiterpenoid from the marine alga *Caulerpa Taxifolia. Anticancer Res.*, **1995**, *15*, 2155.

[7] Barbier, P.; Guise, S.; Huitorel, P.; Amade, P.; Pesando, D.; Briand, C.; Peyrot, V. Caulerpenyne from caulerpa taxifolia has an antiproliferative activity on tumor cell line SK-N-SH and modifies the microtubule network. *Lifes Sci*., **2001**, *70*, 415.

[8] Manfredi, J.J.; Horwitz, S.B. Taxol: an antimitotic agent with a new mechanism of action. *Pharmacol. Ther.*, **1984**, *25*, 83.

[9] Jordan, M.A.; Margolis, R.L.; H.Himes, R.; Wilson L. Identification of a distinct class of vinblastine binding sites on microtubules. *J. Mol. Biol.,* **1986**, *187*, 61-73.

[10] Olmsted, J.B.; Borisy, G.G. Microtubules. *Ann. Rev. Biochem.,* **1973**, *42*, 507.

[11] Loike, J.D.; Brewer, C.F.; Sternlicht, H.; Gensler, W.J. ; Horwitz, S.B. Structure-Activity study of the inhibition of microtubule assembly *in vitro* by podophyllotoxin and its congeners. *Cancer Res.*, **1978**, *38*, 2688.

[12] Owellen, R.J.; Hartke, C.A.; Dickerson, R.M.; Horwitz, S.B. Inhibition of tubulin-microtubule polymerization by drugs of the vinca alkaloid class. *Cancer Res.,* **1976**, *36*, 1499-1502.

[13] Li, Y.; Kobayashi, H.; Hashimoto, Y.; Shirai, R.; Hirata, A.; Hayashi, K.; Hamada, Y.; Shioiri, T. Iwasaki, S. Interaction of marine toxin dolastatin10 with porcine brain tubulin. *Chem. Biol. Int.*, **1994**, *93*, 175.

[14] Huitorel, P.; Pantaloni, D. Bundling of microtubules by glyceraldehydes-3-phosphate dehydrogenase and its modulation by ATP. *Eur. J. Biochem.,* **1985**, *150*, 265.

[15] Peyrot, V.; Briand, C.; Momburg, R.; Sari, J.C. *In vitro* mechanism study of microtubule assembly inhibition by *Cis*-dichlorodiamine-platinum(II). *Biochem. Pharmacol.,* **1986**, *35*, 371.

[16] Carré, M.; Carles, G.; André, N.; Douillard, S.; Ciccolini, J.; Briand, C.; Braguer, D. Involvement of microtubules and mitochondria in the antagonism of arsenic trioxide on paclitaxel-induced apoptosis. *Biochem. Pharmacol*., **2002**, *63*, 1831.

[17] Himes, R.H.; Himes, W.B. Inhibition of tubulin assembly by ethylacetylacrylate, a sulfhydryl reagent and potential analog of cytochalasin A. *Biochim. Biophys. Acta*, **1980**, *621*, 338.

[18] Ponstingl, H.; Krauhs, E.; Little, M.; Kempf, T. Complete amino acid sequence of alpha-tubulin from porcine brain. *Proc. Natl. Acad. Sci. U. S. A.,* **1981**, *78*, 2757.

[19] Barbier, P.; Gregoire, C.; Devred, F.; Sarrazin, M.; Peyrot, V. *In vitro* effect of cryptophycin 52 on microtubule assembly and tubulin: Molecular modelling of the mechanism of action of a new antimitotic drug. *Biochemistry*, **2001**, *40*, 13510.

[20] Leynadier, D.; Peyrot, V.; Sarrazin, M.; Briand, C.; Andreu, J.M.; Rener, G.A.; Temple, C. Jr. Tubulin binding of two 1-deaza-7,8-dihydropteridines with different biological properties: enantiomers NSC 613862 (S)-(-) and NSC 613863 (R)-(+). *Biochemistry*, **1993**, *32*, 10675.

[21] De Ines, C.; Leynadier, D.; Barasoain, I.; Peyrot, V.; Garcia, P.; Briand, C.; Rener, G. A.; Temple, C. Jr. Inhibition of microtubules and cell cycle arrest by a new 1-deaza-7,8-dihydropteridine antitumor drug, CI 980, and by its chiral isomer. *Cancer Res.,* **1994**, *54*, 75.

[22] Barbier, P.; Peyrot, V.; Sarrazin, M.; Rener, G.A.; Briand, C. Differential effects of ethyl 5-amino-2-methyl-1,2-dihydro-3-phenylpyrido[3,4-b]pyrazin-7-yl carbamate analogs modified at position C2 on tubulin polymerization, binding, and conformational changes. *Biochemistry,* **1995**, *34*, 16821.

[23] Allam, N.; Millot, J.M.; Manfait, M.; Leynadier, D.; Peyrot, V.; Briand, C.; Temple, C. Jr. Molecular interaction of tubulin with 1-deaza-7,8-dihydropteridines: a comparative study of enantiomers NSC 613862 (S) and NSC 613863 (R) by Raman and Fourier transform infrared spectroscopy. *Int. J. Biol. Macromol.,* **1995**, *17*, 55.

[24] Barbier, P.; Peyrot, V.; Dumortier, C.; D'Hoore, A.; Rener, G. A.; Engelborghs, Y. Kinetics of association and dissociation of two enantiomers, NSC 613863 (R)-(+) and NSC 613862 (S)-(-) (CI 980), to tubulin. *Biochemistry*, **1996**, *35*, 2008.

[25] Barbier, P.; Peyrot, V.; Leynadier, D.; Andreu, J.M. The active GTP- and ground GDP-liganded states of tubulin are distinguished by the binding of chiral isomers of ethyl 5-amino-2-methyl-1,2-dihydro-3-phenylpyrido[3,4-b]pyrazin-7-yl carbamate. *Biochemistry*, **1998**, *37*, 758.

[26] Peyrot, V.; Barbier, P.; Sarrazin, M.; Briand, C.; Andreu, J.M. Chirality and Spectroscopic Changes Induced by the recognition of Ethyl 5-amino-2-methyl-1,2-dihydro-3-phenylpyrido[3,4-*b*]pyrazin-7-yl carbamate analogs by Tubulin. *Photochem. Photobiol.,* **1999**, *70*, 710.

[27] Ravelli, R.B.; Gigant, B.; Curmi, P.A.; Jourdain, I.; Lachkar, S.; Sobel, A.; Knossow, M. Insight into tubulin regulation from a complex with colchicine and a stathmin-like domain. *Nature*, **2004**, *428*, 198.

[28] Bai, R., Schwartz, R.E., Kepler, J.A., Pettit, G.R., Hamel, E. Characterization of the interaction of cryptophycin 1 with tubulin: binding in the Vinca domain, competitive inhibition of dolastatin 10 binding, and an unusual aggregation reaction. *Cancer Res.,* **1996**, *56*, 4398.

[29] Smith, C.D.; Zhang, X. *J.* Mechanism of action cryptophycin. Interaction with the Vinca alkaloid domain of tubulin. *Biol. Chem.,* **1996**, *271*, 6192.

[30] Panda, D.; Ananthnarayan, V.; Larson, G.; Shih, C.; Jordan, M.A.; Wilson, L. Interaction of the antitumor compound cryptophycin-52 with tubulin. *Biochemistry*, **2000**, *39*, 14121.

[31] Watts, N. R.; Cheng, N.; West, W.; Steven, A.C.; Sackett, D. L. The cryptophycin-tubulin ring structure indicates two points of curvature in the tubulin dimer. *Biochemistry*, **2002**, *41*, 12662.

[32] Howard, W.D.; Timasheff, S.N. Linkages between the effects of taxol, colchicine, and GTP on tubulin polymerization. *J. Biol. Chem*., **1988**, *263*, 1342.

[33] Yoshida, M.; Matsui, Y.; Ikarashi, Y.; Usui, T.; Osada, H.; Wakasugi, H. Antiproliferating activity of the mitotic inhibitor pironetin against vindesine- and paclitaxel-resistant human small cell lung cancer H69 cells. *Anticancer Res*., **2007**, *27*, 729.

[34] Madari, H.; Panda, D.; Wilson, L.; Jacobs, R.S. Dicoumarol: A unique microtubule stabilizing natural product that is synergistic with taxol. *Cancer Res.,* **2003**, *63*, 1241.

[35] Temple, C. Jr.; Rener, G.A. New anticancer agents: chiral isomers of ethyl 5-amino-1,2-dihydro-2-methyl-3-phenylpyrido[3,4-b]pyrazine-7-carbamate. *J. Med. Chem.,* **1989**, *32*, 2089.

[36] Weisenberg, R.C.; Borisy, G.G. Taylor, E.W. The colchicine-binding protein of mammalian brain and its relation to microtubules. *Biochemistry*, **1968**, *1*, 4466.

[37] Peyrot, V.; Andreu, J.M.; Briand, C. C-terminal cleavage of tubulin by subtilisin enhances ring formation. *Arch. Biochem. Biophys*., **1990**, *279*, 328.

[38] Schuck, P.; Rossmanith, P. Determination of the sedimentation coefficient distribution by least-squares boundary modeling. *Biopolymers,* **2000**, *54*, 328.

[39] Andreu, J. M.; Timasheff, S.N. Conformational states of tubulin liganded to colchicines, tropolone methyl ether, podophyllotxin. *Biochemistry*, **1982**, *21*, 6465.

[40] Diaz, F. J.; Andreu, J. M. Assembly of purified GDP-tubulin into microtubules induced by taxol and taxotere: reversibility, ligand stoichiometry, and competition. *J. Biol. Chem.,* **1991**, *266*, 2890.

Received: 09 September, 2008 Revised: 23 December, 2008 Accepted: 12 January, 2009